Taylor & Francis
Taylor & Francis Group

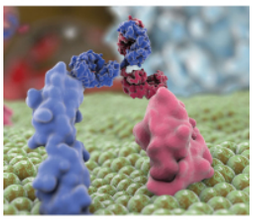

mAbs

ISSN: (Print) (Online) Journal homepage: https://www.tandfonline.com/loi/kmab20

Discovery and characterization of prolactin neutralizing monoclonal antibodies for the treatment of female-prevalent pain disorders

Stephanie Maciuba, Gregory D. Bowden, Harrison J. Stratton, Kazimierz Wisniewski, Claudio D. Schteingart, Juan C. Almagro, Philippe Valadon, Joshua Lowitz, Scott M. Glaser, Grace Lee, Mahdi Dolatyari, Edita Navratilova, Frank Porreca & Pierre J.M. Rivière

To cite this article: Stephanie Maciuba, Gregory D. Bowden, Harrison J. Stratton, Kazimierz Wisniewski, Claudio D. Schteingart, Juan C. Almagro, Philippe Valadon, Joshua Lowitz, Scott M. Glaser, Grace Lee, Mahdi Dolatyari, Edita Navratilova, Frank Porreca & Pierre J.M. Rivière (2023) Discovery and characterization of prolactin neutralizing monoclonal antibodies for the treatment of female-prevalent pain disorders, mAbs, 15:1, 2254676, DOI: 10.1080/19420862.2023.2254676

To link to this article: https://doi.org/10.1080/19420862.2023.2254676

MABS
2023, VOL. 15, NO. 1, 2254676
https://doi.org/10.1080/19420862.2023.2254676

Taylor & Francis
Taylor & Francis Group

REPORT

OPEN ACCESS Check for updates

Discovery and characterization of prolactin neutralizing monoclonal antibodies for the treatment of female-prevalent pain disorders

Stephanie Maciuba[a*], Gregory D. Bowden[a*], Harrison J. Stratton[b], Kazimierz Wisniewski[a], Claudio D. Schteingart[a], Juan C. Almagro[c], Philippe Valadon[d], Joshua Lowitz[e], Scott M. Glaser[a], Grace Lee[b], Mahdi Dolatyari[b], Edita Navratilova[b], Frank Porreca[b], and Pierre J.M. Rivière[a]

[a]Peptide Logic, San Diego, CA, USA; [b]Department of Pharmacology, The University of Arizona, Tucson, AZ, USA; [c]GlobalBio, Cambridge, MA, USA; [d]Antibody Design Labs, San Diego, CA, USA; [e]Antibody Solutions, Santa Clara, CA, USA

ABSTRACT

Prolactin (PRL) has recently been demonstrated to elicit female-selective nociceptor sensitization and increase pain-like behaviors in female animals. Here we report the discovery and characterization of first-in-class, humanized PRL neutralizing monoclonal antibodies (PRL mAbs). We obtained two potent and selective PRL mAbs, PL 200,031 and PL 200,039. PL 200,031 was engineered as human IgG1 whereas PL 200,039 was reformatted as human IgG4. Both mAbs have sub-nanomolar affinity for human PRL (hPRL) and produce concentration-dependent and complete inhibition of hPRL signaling at the hPRL receptor (hPRLR). These two PRL mAbs are selective for hPRL as they do not inhibit other hPRLR agonists such as human growth hormone or placental lactogen. They also cross-react with non-human primate PRL but not with rodent PRL. Further, both mAbs show long clearance half-lives after intravenous administration in FcRn-humanized mice. Consistent with their isotypes, these mAbs only differ in binding affinities to Fcγ receptors, as expected by design. Finally, PL 200,019, the murine parental mAb of PL 200,031 and PL 200,039, fully blocked stress-induced and PRL-dependent pain behaviors in female PRL-humanized mice, thereby providing *in vivo* preclinical proof-of-efficacy for PRL mAbs in mechanisms relevant to pain in females.

ARTICLE HISTORY
Received 5 June 2023
Revised 19 August 2023
Accepted 30 August 2023

KEYWORDS
Antibody; prolactin; pain; sex-selective; women

Introduction

Women have higher sensitivity to experimental pain and are at a greater risk of experiencing many clinical pain syndromes.[1] The most striking sex differences are observed in functional pain syndromes (FPS), a large subgroup of pain conditions defined by the absence of a clear etiology or tissue injury.[2] FPS are characterized by unusually high female:male prevalence ratios. These include, but are not limited to, temporomandibular disorders (9:1 ratio), fibromyalgia (9:1 ratio), irritable bowel syndrome (3:1 ratio), and migraine (3:1 ratio).[3–6] In addition, women are also affected by female-specific pain conditions, such as dysmenorrhea, endometriosis, and vulvodynia.[7–9] Female-predominant FPS and female-specific pain conditions typically peak during reproductive age, are often exacerbated during the menstrual cycle and by stress, and regress or disappear after menopause, suggesting the involvement of stress and/or female hormones in FPS sex disparities.[10–14]

Prolactin (PRL) has recently emerged as a key factor that promotes female-selective nociception and pain-like behaviors in preclinical models.[15–24] Such sexually dimorphic effects are likely to be of high translational relevance in promoting pain in women. PRL is a widely expressed polypeptide hormone exerting pleiotropic endocrine, paracrine, and autocrine functions.[25,26] PRL is produced by lactotroph cells of the anterior pituitary and multiple extra-pituitary tissues.[27] Circulating PRL levels are higher in women than men, increase during reproductive age and under stress, vary during the menstrual cycle, and decline after menopause, suggesting control by female sex hormones.[28,29] PRL plays a critical role in mammogenesis and lactogenesis, and thus is naturally elevated during pregnancy and breastfeeding.[30] Excessive PRL has been associated with galactorrhea, amenorrhea, mastalgia, infertility, endometriosis, osteoporosis, breast and prostate cancer, erectile dysfunction, and migraine.[30–37]

The PRL receptor (PRLR) is expressed in trigeminal ganglion (TG) and dorsal root ganglia (DRG) neurons in rodents, and PRL selectively sensitizes female TG and DRG nociceptors.[15,18–20,38] Furthermore, topical application of PRL to the dura mater produces migraine-like pain in female but not male animals, and is associated with release of calcitonin gene-related peptide, a peptide known to trigger migraine attacks in humans.[15,18,39] Patients with hyperprolactinemia have increased migraine that decreases with treatment of hyperprolactinemia.[31,40–42] Altogether, these data suggest that excessive PRL signaling could contribute to migraine in women, as well as possibly to a broader range of female-predominant FPS or female-specific pain conditions, and that blocking both pituitary and extra-pituitary PRL may be clinically beneficial to treat pain in women.

CONTACT Pierre J.M. Rivière pierre.riviere@peptidelogic.com
*These authors contributed equally to this work.
Supplemental data for this article can be accessed online at https://doi.org/10.1080/19420862.2023.2254676

Both production and secretion of PRL in pituitary and extra-pituitary tissues are differentially regulated.[30,43,44] In humans, there is a single gene coding for PRL and two distinct promoters regulating PRL expression in pituitary and extra-pituitary tissues.[43] Dopamine inhibits PRL secretion from the pituitary but does not affect extra-pituitary PRL.[44] Dopaminergic type 2 (D2) receptor agonists, such as cabergoline or bromocriptine, while useful to inhibit PRL release from the pituitary, do not control PRL release from extra-pituitary tissues.[33,44] Attempts at developing therapeutics able to block both pituitary and extra-pituitary PRL responses have focused on PRLR antagonists, either peptides or PRLR antibodies.[45–47] Previously disclosed peptide PRLR antagonists have been used as pharmacological tools, but they have insufficient potency and their duration of action is too short to enable development as therapeutics.[48,49] Efforts to extend the half-life of these peptide PRLR antagonists by addition of an albumin binding domain resulted in a loss in potency.[50] Furthermore, PRLR antibodies, while effective at inhibiting PRL-induced activation of PRLR, are not selective for PRL, as they also inhibit PRLR activation by growth hormone and placental lactogen, two hormones structurally related to PRL.[51] Currently, there is no medication available that can solely and completely neutralize responses to PRL produced by both pituitary and extra-pituitary sites. Here, we describe novel humanized prolactin neutralizing monoclonal antibodies (PRL mAbs) with high affinity and selectivity for human PRL (hPRL), and the ability to potently and selectively inhibit hPRL activation of the human PRLR (hPRLR).

Results

Identification of the PRL-neutralizing mAb lead

A collection of purified antibodies generated by mouse immunization and hybridoma methods were evaluated for their ability to block hPRL activation of hPRLR in an *in vitro* functional assay. Activation of hPRLR was monitored by measuring intracellular phosphorylated STAT5 in GS Xceed CHOK1SV GS-KO cells stably expressing the long hPRLR isoform using a time-resolved fluorescence energy transfer (TRFRET)-based assay.[26,52] Concentration-response curves for hPRLR activation were generated for hPRL, as well as for human GH (hGH) and human PL (hPL), two related hormones known to also activate hPRLR.[51] hPRL, hGH, and hPL produced concentration-dependent and maximal activation of the hPRLR (Figure 1a) with half-maximal effective concentration (EC_{50}) of 9 nM, 9 nM, and 172 nM, respectively.

Fourteen candidate and three reference monoclonal antibodies (mAbs) were screened for neutralizing activity by pre-incubating the mAbs with a submaximally effective concentration of hPRL prior to the functional assay. Only six of the candidate mAbs and one reference mAb (INNhPRL1) inhibited hPRL activation of hPRLR by ≥ 80% (Figure 1b). The other eight candidates and two reference mAbs (6F11, A7) were either less effective or unable to reduce hPRL response, demonstrating that not all hPRL-binding mAbs prevent hPRL activation of hPRLR.

To identify a lead antibody, the six candidates were further progressed to full concentration-response curve studies to assess their abilities to inhibit the agonist activity of hPRL at the hPRLR. All candidates displayed a concentration-dependent and complete inhibition of hPRLR activation by hPRL (Supplementary Figure S1). The most potent mAb candidate had a half-maximal inhibitory concentration (IC_{50}) of 2.1 nM (Supplementary Table S1), displayed complete inhibition of hPRLR activation at half the molar concentration of hPRL in the assay, and was selected as a lead for subsequent characterization.

Characterization of PL 200,019

To support further characterization, the murine mAb lead from the previous screen was recombinantly expressed using Lonza's GS Xceed Expression System in a fed-batch production, protein G purified, and analytically characterized. The resulting product, PL 200,019, exhibited

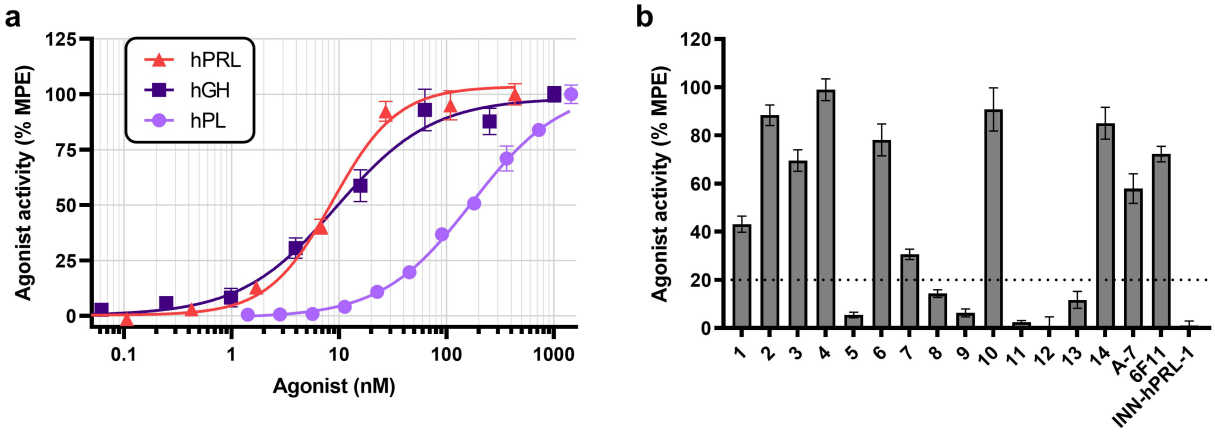

Figure 1. Screen for hybridoma-derived mAbs with hPRL-neutralizing activity. (a) hPRLR-expressing CHOK1SV GS-KO cells were stimulated with increasing concentrations of hPRL (0–434 nM), hGH (0–1,010 nM), or hPL (0–1,449 nM) for 15 minutes at 37°C before measuring hPRLR signaling by phospho-STAT5 TR-FRET activity assay. Data was normalized to maximum response observed for each agonist. Values represent mean ± SEM of two (hPL) or three independent experiments (hPRL and hGH). (b) hPRLR-expressing CHOK1SV GS-KO cells were stimulated with 20 nM hPRL preincubated with 100 nM of various hybridoma-derived mAbs or control mAbs with reported PRL-neutralizing activity. Data was normalized to maximum response of untreated stimulated cells. Values represent mean ± SEM of two independent screens. The dotted horizontal line represents 80% inhibition cutoff.

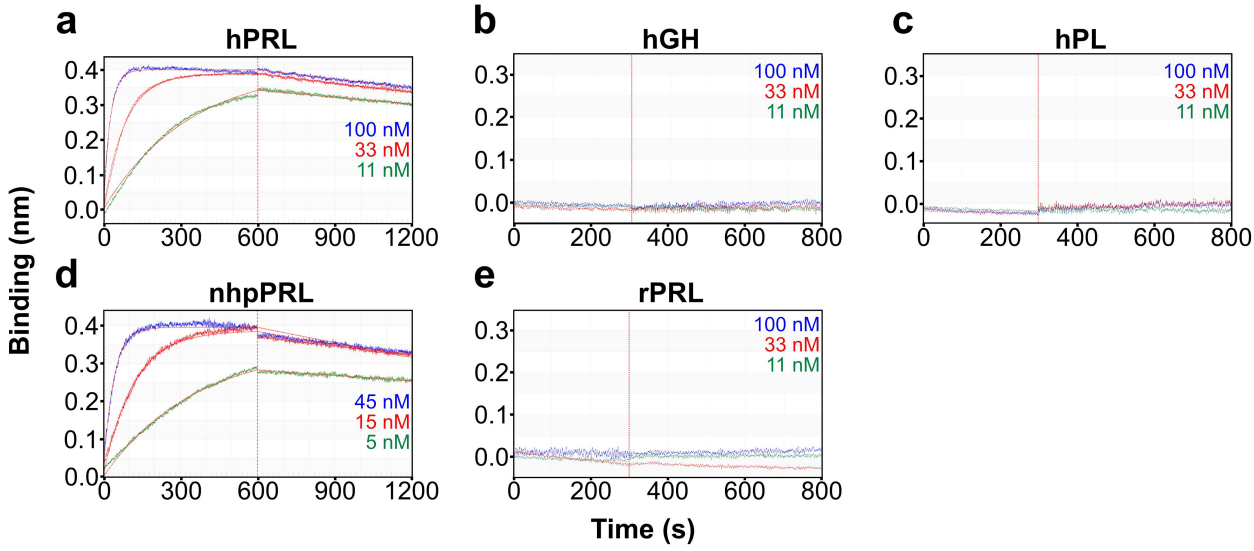

Figure 2. Binding kinetics of PL 200,039. Biolayer interferometry analysis of the binding of PL 200,039 to (a) hPRL, (b) hGH, (c) hPL, (d) nhpPRL, and (e) rPRL accomplished by immobilizing PL 200,039 onto anti-human-Fc capture biosensors, and incubating a range of concentrations (100, 33, 11 nM or 45, 15, 5 nM) of each analyte. Kinetic parameters were calculated using a 1:1 model with global fitting. Experimental response at each concentration are shown with each calculated fitted curve (solid lines).

comparable efficacy and potency to the hybridoma-purified mAb in inhibiting hPRL activation of hPRLR. As expected, PL 200,019 did not inhibit hGH or hPL responses (Supplementary Figure S2a), thus confirming selectivity for hPRL and lack of cross-reactivity with other hPRLR agonists. This further demonstrated that the observed neutralizing activity of PL 200,019 is a result of binding to hPRL and not hPRLR. Furthermore, PL 200,019 inhibited non-human primate PRL (nhpPRL) activation of hPRLR (Supplementary Figure S2c, IC_{50}: 5.8 nM), but not mouse PRL (mPRL) or rat PRL (rPRL) activation of the mouse PRL receptor (mPRLR), thereby establishing species cross-reactivity with primate but not rodent PRL (Supplementary Figure S2d). PL 200,019 is a mouse IgG1/kappa with a IGHV1–9 × 01 variable heavy chain and a IGKV3–5 × 01 variable light chain. Based on these results, PL 200,019 was further progressed to humanization.

Humanization and candidate selection

PL 200,019 complementarity-determining regions (CDRs) were grafted onto four human variable heavy (VH) and four human variable light (VL) region frameworks (*i.e.*, a 4 × 4 matrix). All 16 VH and VL combinations were transiently expressed as human IgG1 in HEK293T cells and assayed for binding to hPRL by direct enzyme-linked immunosorbent assay (ELISA) (data not shown). The developability properties of all humanized mAbs were compared to commercially available therapeutic mAbs *in silico* (Supplementary Table S2) and the top six candidates were screened *in vitro* in the hPRL/hPRLR functional assay (data not shown). The resulting PRL mAb with the best overall profile, PL 200,031, achieved a potency comparable to its parent murine mAb (IC_{50} of 2.7 nM *vs.* 3.2 nM, respectively, data not shown) and did not exhibit any development liabilities. PL 200,031 was reformatted as a human IgG4 with S228P hinge stabilizing mutation to generate PL 200,039, a PRL mAb variant with expected reduced antibody effector functions.[53,54]

Stable CHOK1SV GS-KO cell pools expressing PL 200,031 and PL 200,039 were generated using Lonza's GS Xceed Expression System. Both stable pools regularly reached ≥3 g/L expression yield in non-optimized, research-grade fed-batch production, suggesting that after further cell line development, clonal selection, and optimization of bioreactor culture conditions, both antibodies would likely achieve significantly higher yields during large-scale GMP manufacturing. Production of the PRL mAbs yielded a uniform, monomeric product of expected size following purification (Supplementary Figures S3 and S4, Supplementary Tables S3 and S4). Additionally, both PRL mAbs were able to be concentrated to >100 mg/ml in 20 mM, pH 6.0 histidine buffer without apparent aggregation (Supplementary Table S5). The IgG1-based PL 200,031 and IgG4-based PL 200,039 were selected as PRL mAb leads and evaluated jointly in subsequent comparative studies.

Binding affinity of PL 200,031 and PL 200,039

Binding kinetics and affinities of PL 200,019, PL 200,031, and PL 200,039 for hPRL were first determined by biolayer interferometry. The representative sensorgrams for PL 200,039 are shown in Figure 2. All antibodies showed strong, sub-nanomolar affinity for hPRL (Table 1). The binding kinetics of PL 200,039 for nhpPRL, rPRL, hGH, and hPL were also assessed. As expected, PL 200,039 maintained strong affinity for nhpPRL and did not display any significant binding to rPRL, hGH, or hPL, highlighting its selectivity for primate PRL (Table 1).

Table 1. Kinetic rate constants and equilibrium dissociation constants for the binding interactions of lactogenic hormones with PRL mAbs. If binding was not observed, rates are labeled as not detected (n.d.).

ID	Class	Antigen	$k_{on}(M^{-1} \cdot s^{-1})$	k_{off} (s^{-1})	K_D (pM)
PL 200,019	Murine IgG1	hPRL	8.2×10^5	8.1×10^{-5}	99
PL 200,031	Humanized IgG1	hPRL	2.7×10^5	7.2×10^{-5}	268
PL 200,039	Humanized IgG4 (S228P)	hPRL	3.5×10^5	2.2×10^{-4}	630
		hGH	n.d.	n.d.	n.d.
		hPL	n.d.	n.d.	n.d.
		nhpPRL	5.4×10^5	3.1×10^{-4}	570
		rPRL	n.d.	n.d.	n.d.

Table 2. Inhibition of PRLR signaling by PRL mAbs.

		IC_{50} (nM)				
ID	Class	hPRL	hGH	hPL	nhpPRL	rPRL
PL 200,019	Murine IgG1	2.7	>150	>2,600	3.2	>150
PL 200,031	Humanized IgG1	2.8	>150	>2,600	3.0	>150
PL 200,039	Humanized IgG4(S228P)	3.6	>150	>2,600	5.3	>150

Data are presented as geometric means of three independent experiments. IC50: half-maximal inhibitory concentration.

Neutralizing activity and selectivity of PL 200,031 and PL 200,039

To confirm that the humanized mAbs PL 200,031 and PL 200,039 maintained selective neutralization of hPRL, their activities were compared to the parental murine mAb PL 200,019 in the hPRLR functional assay. Both antibodies produced a potent, concentration-dependent, and complete inhibition of both hPRL- and nhpPRL-induced activation of hPRLR, but did not inhibit hGH- and hPL-induced activation of hPRLR, or rPRL-induced activation of mPRLR (Table 2, Figure 3, Figure S5). These functional data were consistent with the above binding data and demonstrated that PL 200,031 and PL 200,039 selectively bind and inhibit hPRL response without altering responses to other known hPRLR agonists. Further, these results confirm that PL 200,031 and PL 200,039 cross-react with non-human primate but not rodent PRL, which is critical for selection of the relevant species for pharmacology, safety, and toxicology studies.

The epitope bound by humanized PRL mAbs was determined using crosslinking and mass spectrometry (data not shown). While the determined epitope region does not overlap with key receptor-binding residues, it is sufficiently close in proximity that binding of an antibody would likely prevent binding to the receptor. Overall, our initial data suggest that PRL mAbs inhibit hPRL by sterically impeding its binding to hPRLR.

Fc domain-mediated functions of PL 200,031 and PL 200,039

Engagement of fragment crystallizable (Fc) gamma receptors (FcγRs) by antibodies can initiate the Fc-mediated effector functions of antibody-dependent cellular cytotoxicity (ADCC) and antibody-dependent cellular phagocytosis (ADCP).[55] To evaluate the ability of PRL mAbs to initiate effector functions, we assessed binding of PL 200,031 and PL 200,039 to the primary activating FcγRs (FcγRI, FcγRIIA, and

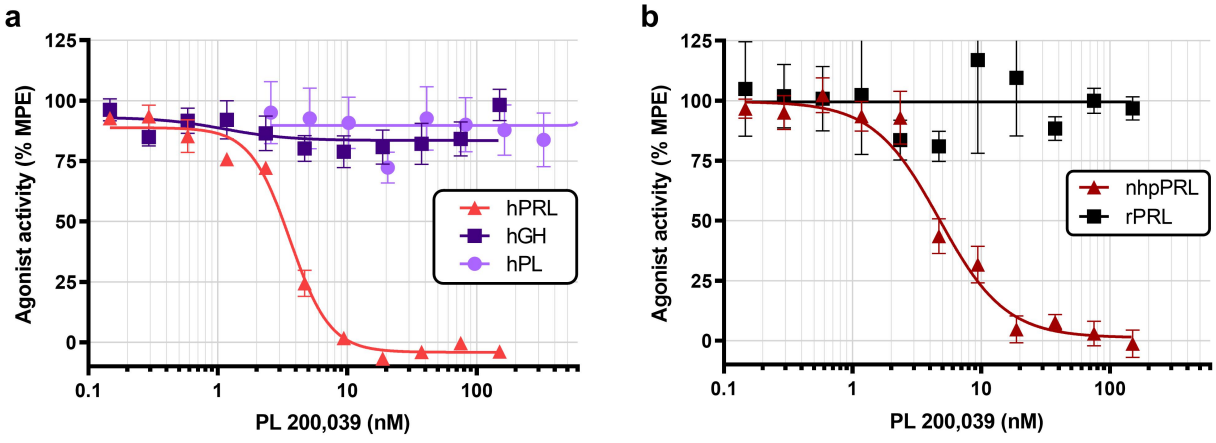

Figure 3. Selectivity and cross-reactivity of PL 200,039. (a) hPRLR-expressing CHOK1SV GS-KO cells were stimulated for 15 minutes at 37°C with constant 20 nM hPRL, 20 nM hGH, or 350 nM hPL preincubated with varying concentrations (0–150 nM or 0–2.6 µM) of PL 200,039 for 30 minutes prior to stimulation. Data was compiled from three independent experiments and normalized to response of cells stimulated in the absence of antibody. Values represent mean ± SEM. (b) CHOK1SV GS-KO cells expressing hPRLR or mPRLR were stimulated as before with constant 20 nM nhpPRL or 20 nM rPRL, respectively, preincubated for 30 minutes with varying concentrations (0–150 nM) of PL 200,039 prior to stimulation. Data was compiled from two (rPRL) or three (nhpPRL) independent experiments and normalized to the response of cells stimulated in the absence of antibody. Values represent mean ± SEM.

Table 3. Competitive binding of PRL mAbs to FcγRs by immunoassay.

	IC_{50} (nM)				
Antibody	FcγRI	$FcγRIIA_{H131}$	$FcγRIIA_{R131}$	$FcγRIIIA_{F158}$	$FcγRIIIA_{V158}$
PL 200,031	0.23	55	92	95	3.0
PL 200,039	0.96	>5,000	1,900	>5,000	3,800
hIgG1 Control	0.33	12	27	110	5.9
hIgG2 Control	>5,000	23	>5,000	>5,000	>5,000
hIgG4 Control	2.0	270	230	>5,000	1,600

Data represents the mean of triplicate experiments. Half-maximal inhibitory concentration (IC_{50}) values were calculated from the curves shown in Supplementary Figure S6.

FcγRIIIA, with accompanying allotypes) by immunoassay (Supplementary Figure S6). As expected, IgG4 PL 200,039 performed comparably to the IgG4 isotype control and demonstrated a significant reduction in IC_{50} for allotypes of FcγRIIA and FcγRIIIA when compared to IgG1 PL 200,031, while retaining binding to FcγRI (Table 3).

Pharmacokinetic profile of PL 200,031 and PL 200,039

PL 200,031 and PL 200,039 pharmacokinetic (PK) profiles were evaluated in male FcRn-humanized mice (Tg32) after administration of a single dose (5 mg/kg) by intravenous (IV) route in the tail vein (5 mL/kg).[56] Blood samples were collected at various time points over a 28-day period, processed to plasma, and analyzed by ELISA. PL 200,031 and PL 200,039 had comparable PK profiles (Figure 4), with elimination half-life of 13.1 and 15.7 days, respectively.

Efficacy of a PRL mAb in stress-related pain in female mice

Previous studies have demonstrated that mPRL induces female-selective pain in mice.[15,16,20–22,39,57] Specifically, we previously demonstrated that restraint stress (RS) induced an increase in circulating PRL that was associated with both periorbital and extracephalic (data not shown) allodynia in female wildtype mice.[38] The D2 agonist cabergoline blocked RS-induced PRL release as well as periorbital and extracephalic (data not shown) allodynia, thus demonstrating involvement of pituitary mPRL in this model of female pain in wildtype mice.[38]

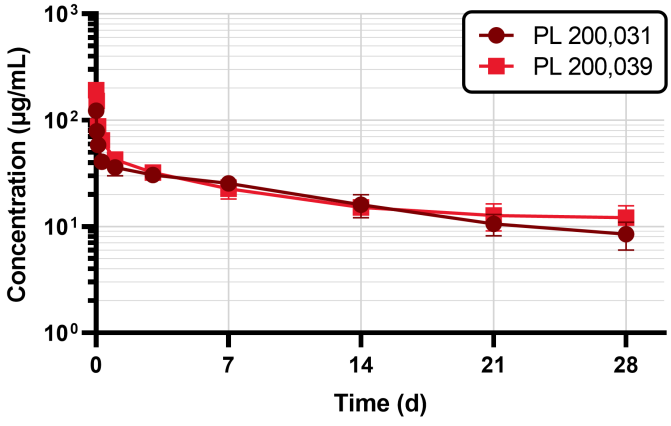

Figure 4. Pharmacokinetic profile of PL 200,031 and PL 200,039 after single dose (5 mg/kg) IV administration in FcRn-humanized Tg32 mice. Data represents mean serum concentrations ± SD from each group ($n = 3$).

Wildtype mice, however, are not suitable to determine the efficacy of PRL mAb leads as they do not cross-react with mPRL. We thus established a new colony of a previously characterized PRL-humanized mouse that expresses hPRL instead of mPRL (B6.Cg-Prl^{tm1Hmn} Tg(PRL)30Greg/Mmmh).[58] Previous characterization of this PRL-humanized mouse indicated that hPRL expression and regulation as well as reproductive functions were comparable to wildtype mice.[58] This is in agreement with separate studies demonstrating that hPRL is a potent and full agonist at the mPRLR.[58,59] Therefore, the PRL-humanized mouse is an appropriate model to study the efficacy of PRL mAbs in PRL-dependent pain models. To prevent the possibility of undesired immune responses and a short half-life, which are often observed when human mAbs are administered to mice, we elected to use PL 200,019, the murine parent of the PRL mAbs.

We first confirmed that the PRL-humanized mouse strain (hPRL$^{+/+}$, mRPL$^{-/-}$) expresses hPRL and not mPRL (Figure 5a), using PRL ELISA kits that distinguish between hPRL and mPRL. We further confirmed that repeated 2-hour RS for three consecutive days induced hindpaw mechanical allodynia in female PRL-humanized mice (Figure 5b). Subcutaneous (SC) administration of PL 200,019 fully blocked stress-induced allodynia in female PRL-humanized mice (Figure 5b), thereby establishing proof-of-efficacy for PRL mAbs in an animal model of PRL-dependent female pain.

Discussion

Here we report the discovery, engineering, and characterization of two first-in-class, humanized PRL mAbs, PL 200,031 and PL 200,039. The former is a human IgG1 whereas the latter is a human IgG4. PL 200,031 and PL 200,039 have both subnanomolar affinity for hPRL and produce concentration-dependent and potent inhibition of hPRL activation of the hPRLR *in vitro*. PL 200,031 and PL 200,039 produced complete inhibition of the PRL response at a molar concentration 2-fold lower than PRL concentration (*i.e.*, 1:2 molar ratio) (Figure 3), thus demonstrating that these PRL mAbs have already achieved the maximum possible PRL neutralization activity for this drug class *in vitro*. Most importantly, PL 200,031 and PL 200,039 are both highly selective for hPRL, as demonstrated by the lack of affinity and neutralizing activity against hGH or hPL, two related polypeptide hormones with agonist activity at hPRLR. PL 200,031 and PL 200,039 had similar PK profiles after a single IV administration in FcRn-humanized mice, achieving long elimination half-lives comparable to reference IgG1 and IgG4 therapeutic antibodies in the same FcRn-

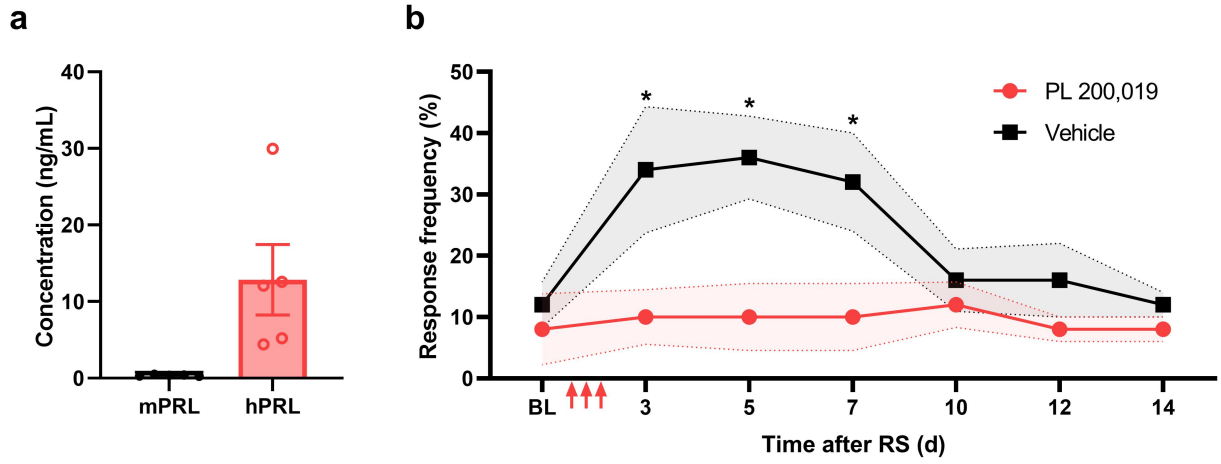

Figure 5. Treatment with PL 200,019 blocks stress-induced mechanical hypersensitivity in female PRL-humanized mice. (a) measurement of PRL in five female PRL-humanized mice using species-specific ELISA. Data presented as mean value for each animal and overall mean ± SEM. (b) stress-induced mechanical hypersensitivity measurement in female PRL-humanized mice treated with PL 200,019 (20 mg/kg) or vehicle ($n = 5$ per group). Baseline mechanical sensitivity (BL) was measured prior to two hours of restraint stress (RS) repeated for three consecutive days (marked by arrows). Data presented as mean ± SEM. *$p < 0.05$ (two-way ANOVA).

humanized mouse model.[56,60] It is unlikely that there will be differences in PK between sexes as the FcRn receptor, the primary factor regulating mAb PK, is identical in males and females. However, considering the targeted patient population, subsequent PK evaluations in non-human primates (NHPs) and humans will focus on female subjects.

As mAb PK data obtained in the FcRn-humanized mouse have demonstrated good predictivity and translatability to higher species, we project that PL 200,031 and PL 200,039 will also achieve long half-lives in both NHPs and humans.[61–63]

We initially considered both IgG1 and IgG4 formats only to keep both options open from a safety perspective. PRL is a circulating hormone as opposed to a cell surface antigen and therefore, a priori, an unlikely substrate for cell-mediated Fc effector function (e.g., ADCC, ADCP) or CDC. Nevertheless, we pursued both isotype formats in parallel as we experimentally analyzed study results for any potential indication of indirect unwanted activity. Importantly, our data confirmed that once bound to a PRL mAb, PRL can no longer activate cell surface PRLRs as shown by loss of activity in functional assays, and also strongly supported that PRL can no longer bind cell surface PRLRs due to the mAb steric hindrance as shown in the epitope mapping study. As a result, PRL mAbs, or their immune complexes, are most unlikely to selectively bind either directly or indirectly target cells. For these reasons there is no imperative need to reduce Fc effector functions. Either an IgG1 and or IgG4 format could be equally considered acceptable, pending further investigation.

The high selectivity for hPRL, demonstrated by the lack of affinity and neutralizing activity against hGH or hPL, is a key feature that distinguishes PRL mAbs from previously developed PRLR mAbs, *e.g.*, LFA102 and BAY 1,158,061.[46,47] These two PRLR mAbs have different mechanisms of action (MOA) for inhibiting PRL signaling. LFA102 competitively inhibits binding of hPRL to hPRLR, while BAY 1,158,061 prevents hPRLR activation.[46,47,64] Nonetheless, based on their MOA, these two PRLR mAbs are both likely to indiscriminately block hPRL, hGH and hPL responses at hPRLR, which may lead to unforeseen adverse effects. For instance, PRLR knock-out impedes adipose tissue formation in mice whereas PRL knock-out mice have an unaltered metabolic phenotype.[65,66] Unlike PRLR mAbs, PRL mAbs have the unique potential to selectively ablate PRL-dependent pathogenic processes without impairing naturally-occurring physiological processes driven by other PRLR agonists.

Most importantly, we report for the first time that SC administration of a hPRL-neutralizing antibody (PL 200,019, *i.e.*, the murine analog to PL 200,031 and PL 200,039) prevented stress-induced pain in female PRL-humanized mice, supporting the development of this new drug class in PRL-dependent female pain conditions. These data are clinically relevant since stress-induced PRL release is observed both in humans and in animals, with a higher magnitude in females as compared to males.[28,38] Elevated circulating PRL is associated with migraine in humans and periorbital allodynia (*i.e.*, migraine-like pain) and extracephalic allodynia in female mice.[31,38] Furthermore, treatment with D2 agonists inhibits hyperprolactinemia and associated migraine in humans[31] and stress-induced PRL release and periorbital and extracephalic allodynia in female mice.[38] Collectively, these data demonstrate that dysregulation of pituitary PRL may contribute to female-selective migraine-like pain and possibly other female-prevalent or female-specific pain conditions, and that PRL mAbs are likely to be clinically effective in these PRL-dependent pain conditions. The strong correlation between animal models and clinical observations suggests a high likelihood of translatability and therapeutic success. In addition, extra-pituitary PRL has also been shown to be associated with female pain conditions, including postoperative pain and endometriosis pain.[21,67] Ongoing studies are evaluating the efficacy of PRL mAbs in female pain models dependent on extra-pituitary PRL.

Additionally, considering that PRL is widely expressed and exerts pleiotropic functions, it is likely that PRL mAbs could also be useful in a broad range of indications beyond female pain.[25,26] This includes clinically validated indications

associated with hyperprolactinemia such as amenorrhea, oligomenorrhea, and infertility in women, galactorrhea both in women and men, and impotence in men.[68] In these indications, a PRL mAb would be expected to be safer and better tolerated than currently approved dopaminergic agonists such as cabergoline, which can cause uncontrolled hypertension, cardiac valvulopathy, and fibrosis, and have led the US Food and Drug Administration (FDA) to issue contraindications and warnings for this drug class.[69] It is also reasonable to speculate that PRL mAbs could potentially be useful in other emerging and still untapped indications. For instance, PRL is elevated in systemic lupus erythematosus (SLE), with hyperprolactinemia reported in 15 to 30% of SLE patients. PRL has also been shown to aggravate disease activity in autoimmune diseases animal models.[70] Further, a minority of SLE patients (5% to 6.7%) developed PRL autoantibodies, but there was no statistical relationship between anti-PRL autoantibodies and lupus activity, which is not surprising considering that these autoantibodies lack PRL neutralizing activity.[70–72] Collectively, these data suggest that PRL mAbs could potentially be useful in autoimmune diseases and SLE, contingent to further validation of the MOA in relevant models.

Required safety and toxicology studies in relevant species (NHP) for the Investigational New Drug application (IND) will determine whether prolonged blockade of both pituitary and extra-pituitary PRL responses by a PRL mAb produces safety and/or toxicology concerns that might impact conditions and/or duration of use in the clinic. These studies will determine whether PRL mAbs are suitable for chronic use or whether they should be restricted to short-term use, and whether they should be contraindicated in some circumstances. In the meantime, the FDA review of the safety and toxicology studies for the D2 agonist cabergoline provides useful insight regarding the potential impact of continuous blockage of pituitary PRL secretion.[73] Cabergoline was approved for chronic use, without limitation, except for D2 agonist class specific contraindications and warnings that will not apply to PRL mAbs.[69]

It should also be noted that the high protein concentration that could be achieved with both PL 200,031 and PL 200,039 combined with the positive efficacy results obtained with murine mAb suggest that the humanized mAbs may have suitable attributes for development for SC delivery, an important factor in convenience and patient compliance.

In summary, PL 200,031 and PL 200,039 are both promising candidates for development, offering the desired PK and pharmacodynamics profiles, adequate physicochemical properties, lack of development liabilities confirmed by multiple *in silico* methods, and high expression levels in relevant and predictive recombinant production systems for large scale manufacturing.

Materials and methods

Recombinant proteins

Recombinant human, cynomolgus monkey, and rat PRL were expressed in *E. coli*. Expression plasmids were generated by subcloning genes into pMAL-c6T vector (NEB, #N0378S) to generate N-terminal maltose-binding protein (MBP) fusion proteins. BL21(DE3) competent *E. coli* (Thermo Fisher, #EC0114) were transformed with final expression plasmids. Cultures were grown at room temperature in Luria-Bertani broth supplemented with 0.2% glucose and 100 µg/mL carbenicillin before inducing with 0.3 mM isopropyl β-D-1-thiogalactopyranoside. Cells were harvested, lysed by sonication, and extract was collected by centrifugation. Proteins tagged with MBP were purified from extract using a MBPTrap column (Cytiva, #28918778) and ÄKTA pure automated chromatography system. MBP-tagged PRL was eluted with 20 mM maltose. Fractions were pooled and 3 mM reduced glutathione and 0.3 mM oxidized glutathione were added to encourage disulfide bond formation. Folding was tracked using an Agilent 1100 analytical high performance liquid chromatography (HPLC) system equipped with a MABPac™ reversed phase column (Thermo Fisher, #088644). Following folding, the MBP tag was cleaved from PRL by adding TEV protease (NEB, #P8112S) and incubating at 30°C for 5 hours. Cleavage efficiency was tracked by HPLC. Untagged PRL was isolated by size exclusion chromatography (SEC) using a Superdex 200 Increase 10/300 GL column (Cytiva, #28990946). Additionally, hPRL (R&D Systems, #682-PL-050), mPRL (R&D Systems, #1445-PL-050/CF), hGH (R&D Systems, #1067-SH-025/CF) and hPL (R&D Systems, #5757-PL-025/CF) were used for *in vitro* activity and kinetics assays.

PRLR cell line development

hPRLR (Origene, #RC209266) and mPRLR open reading frames were subcloned into a single gene GS expression vector (Lonza). CHOK1SV GS-KO cells stably expressing hPRLR (GenBank ID NM_000949) or mPRLR (GenBank ID NM_011169.5) were generated using Lonza's GS Xceed Expression System.

Generation of PRL mAbs

Hybridoma culture supernatants prepared from mice immunized with recombinant hPRL were screened for binding to hPRL by ELISA. Selected candidates were expanded for larger-scale antibody production.

ELISA binding assays

Wells of immunoassay plates were coated with target protein solutions in phosphate-buffered saline (PBS) at 4°C overnight and blocked with 1% bovine serum albumin in PBS for one hour at 37°C. After washing with PBS supplemented with 0.05% Tween-20 (PBST), serial dilutions of culture supernatant or purified antibody were added for one hour at 37°C. Unbound analyte was removed by washing three times with PBST. Antibodies bound to target protein were detected by incubating wells with goat anti-mouse or anti-human IgG horse radish peroxidase-conjugated antibodies (Abcam, #ab6789 and #ab97175, respectively) for one hour at 37°C. Excess detection antibody was removed by washing with PBST as before and peroxidase activity was measured using tetramethylbenzidine substrate (Thermo Fisher, #34021)

for 5–10 min before stopping by adding 2 M H_2SO4 and reading absorbance at 450 nm using a TECAN SPARK multimode plate reader.

Humanization

PL 200,019 CDRs were grafted onto four different human variable heavy (VH) and four different human variable light (VL) region frameworks (i.e., a 4 × 4matrix). The four human VH framework germlines genes used were IGHV1–46, IGHV1–69, IGHV1–3, IGHV1–46 × 01/4 m) whereas the four human VL framework genes used were IGKV7–3, IGKV4–1, IGKV1–39, IGKV7–3 × 01/4 m). The VL and the VH domains were cloned in the expression vectors TGEX-LC-hK-Zeo and TGEX-HC-hG1-Zeo (Antibody Design Labs), respectively. Following transient transfection of all 16 HC and LC combinations into HEK 293 cells, supernatants were assayed for binding to hPRL by direct ELISA. Purified antibodies were also screened for neutralization of hPRL activation of hPRLR by *in vitro* activity assay. Humanized antibodies with CDRs derived from the parental murine antibody, utilizing the IGHV1–3 or IGHV1–46 HC human framework and IGKV1–39 or IGKV4–1 human LC framework, were chosen for further development. cDNA sequences for the selected variable regions with IgG1 or IgG4 (with S228P hinge stability mutation)[74,75] HC constant regions were cloned into GS expression vectors (Lonza).[53,54] The S228P IgG4 mutation is effective to prevent undesirable Fab arm exchange with endogenous IgG4 *in vivo* and has previously been used successfully in approved IgG4 antibodies.[76,77]

Antibody expression and purification

Antibodies were expressed either transiently in HEK 293 cells after co-transfection of separate HC and LC expression vectors or were expressed stably in GS Xceed CHOK1SV GS-KO cells (Lonza) after transfection of a single vector that incorporated the DNA sequence of both the HC and LC. Media was harvested from 6-day transient HEK 293 cultures and 15-day CHOK1SV GS-KO fed-batch cultures, clarified by centrifugation and filtration, and purified by Protein A chromatography. Antibodies bound to Protein A resin were eluted using a low pH buffer and neutralized using 1 M Tris/HCl pH 9.0. The final purity of each batch was evaluated using analytical SEC and liquid chromatography-mass spectrometry (LCMS) analysis. Purified antibodies were stored in PBS, pH 7.4 at 4°C.

PRLR cell signaling transduction assay

Agonist-induced PRLR activity was monitored using the THUNDER Phospho-STAT5 (Y694/Y699) TR-FRET Cell Signaling Assay Kit (Bioauxilium, #KIT-STAT5P). In brief, CHOK1SV GS-KO-PRLR cells were plated at 100,000 cells per well in white, low-volume 384 well assay plates. The plated cells were then treated with agonist in triplicate. The assay plates were sealed with porous plate sealer and incubated for 15 minutes at 37°C. Following incubation, cells were lysed by adding lysis buffer supplemented with phosphatase inhibitor cocktail (Bioauxilium) to each well, resealed and incubated for 30 minutes at room temperature with gentle shaking. After lysis, detection antibodies (Bioauxilium) were added to each well. Assay plates were sealed and incubated at room temperature overnight while protected from light. Following incubation, TR-FRET signal was measured at 620 nm and 665 nm excitation using a TECAN SPARK multimode plate reader.

To screen antibodies for their ability to neutralize PRLR agonist activity, cells were treated with agonist in the presence or absence of antibody. Antibodies were pre-incubated with agonist for 30 minutes at room temperature. Cells were then treated with the antibody-PRL mixture in triplicate. hPRL, hGH, nhpPRL, and rPRL were added at a consistent 20 nM dose. For the initial screen, antibodies were added at a consistent 100 nM dose. Control antibodies included in the screen were A-7 (Santa Cruz Biotechnology, #sc -46,698), 6F11 (QED Bioscience, #12205), and INN-hPRL-1 (Abcam, #ab11301). For concentration-response curves, the dose range of antibody was 0–150 nM. For hPL, agonist was added at a consistent 350 nM, and antibody dose range was 0–2.62 μM. Culture medium alone was used as a no treatment control. The IC_{50} of each antibody for each agonist was estimated using the four-parameter logistic regression analysis of GraphPad Prism v9.4.1 (GraphPad Software, San Diego, CA).

Biolayer interferometry for kinetics

Binding kinetics between purified antibodies and various antigens were evaluated by biolayer interferometry on the ForteBio Octet Red96. Purified antibody was immobilized onto ForteBio Anti-Human-Fc Capture biosensors (5 μg/mL), followed by quenching of the biosensors with irrelevant human IgG (150 μg/mL). After a baseline step, real-time measurement of the association and dissociation of antigen was performed at three concentrations (100, 33, 11 nM or 45, 15, 5 nM). On rates (k_{on}), off rates (k_{off}), and the overall equilibrium dissociation constant (K_D) for antibody binding to each concentration of antigen were calculated using the 1:1 model of ForteBio Data Analysis software. A 1:1 Global K_D fit was also performed across multiple concentrations of each antigen.

FcγR binding immunoassays

FcγR binding of PRL mAbs or human IgG1 (Syd Labs Inc., #PA007125), IgG2 (Syd Labs Inc., #PA007127), and IgG4 (S228P) (Syd Labs Inc., #PA007128) isotype controls were estimated using NanoBiT FcγR binding immunoassays (Promega) as described previously.[78] Briefly, serial dilutions of each antibody were co-incubated with recombinant, biotin-labeled FcγRs (FcγRI, $FcγRIIA_{H131}$, $FcγRIIA_{R131}$, $FcγRIIIA_{F158}$, $FcγRIIIA_{V158}$) tagged with streptavidin-SmBiT partial luciferase enzyme in the presence of tracer IgG conjugated to the LgBiT partial luciferase enzyme for 30 minutes at room temperature in wells of white 384-well plates. In the absence of exogenous antibody competition, the interaction between the IgG-LgBiT and SmBiT-labeled FcγR facilitates the formation of a functional NanoBiT luciferase enzyme. After incubation, furimazine luciferase substrate (Promega) was added to each well, and the bioluminescence signal (RLU) was measured

after stabilizing for 3 minutes using a TECAN SPARK multimode plate reader. RLU data was normalized by assigning the maximum RLU in the absence of competing antibody as 100%, and the percentage decrease in signal in the presence of test antibody was calculated. The IC_{50} of each antibody for each FcγR immunoassay was estimated using the four-parameter logistic regression analysis of GraphPad Prism v9.4.1 (GraphPad Software, San Diego, CA).

Physicochemical profiling

Analytical chromatography

SEC analysis was performed on Agilent 1100 HPLC system equipped with an AdvanceBio SEC 300 Å column (Agilent, # PL1580–3301), 4.6 × 150 mm, 2.7 µm. An isocratic elution at 0.3 mL/minute/30°C with 150 mM, pH 7.0 phosphate buffer was used. An Agilent AdvanceBio SEC 300 Å Protein Standard (Agilent, #5190–9417) was used as a reference.

Reverse phase chromatography (RPC) analysis was performed on Agilent 1100 HPLC system equipped with a MAb Pac™ Reversed Phase column (Thermo Fisher, # 088644), 3.0 × 100 mm, 4 µm. A gradient elution from 35% B to 50% B in 10 minutes at 0.7 mL/minute/80°C was used. Buffer A was 0.1% trifluoroacetic acid (TFA) and buffer B was 90% acetonitrile, 0.1% TFA.

Mass spectrometry

PRL mAb samples were analyzed in their intact or reduced form. The reduced samples were obtained by treating the intact samples with tris(2-carboxyethyl)phosphine for one hour at 57°C. An Agilent 6230 time-of-flight mass spectrometer with Jet Stream electrospray ionization source was used for LCMS analysis. The analyses were performed at UCSD Molecular Mass Spectrometry Facility.

Preliminary solubility determination

Approximately 25 mg of an antibody was buffer-exchanged to the 20 mM, pH 6.0 histidine buffer on Amicon Ultra − 2 mL, 30K MWCO centrifugal filter units (Merck Millipore, #UFC203024). The spinning continued at 3,800 rpm until no further changes in volume were observed. The concentrated samples were diluted 50-fold and the concentrations were determined using a Nanodrop Lite spectrophotometer (Thermo Fisher Scientific).[79]

In silico characterization and developability assessment

Paired VL and VH sequences of PL 200,039 and comparative approved therapeutic antibodies were modeled using ABodyBuilder2[80] and submitted to Therapeutic Antibody Profiler[81] for identification of potential liabilities and calculation of five developability parameters. Mean humanness of antibody VL and VH sequences was estimated using T20 score analyzer.[82] The theoretical isoelectric point of antibodies were calculated using the Henderson-Hasselbalch equation described by Kozlowski[83] and pKa values published by Grimsley et al.[84]

Pharmacokinetic study in humanized mice

In a single-dose PK study, B6.Cg-*Fcgrt*^{tm1Dcr} Tg(FCGRT) 32Dcr/DcrJ (Tg32, JAX #014565) mice (three male animals per group) received 5 mg/kg PL 200,031 or PL 200,039 formulated in PBS pH 7.4 by IV administration. Blood samples were collected several times over a 28-day period. Samples were processed to plasma, diluted 1:10 in 50% glycerol in PBS, and stored at −20°C until analysis. Antibody concentrations in serum were measured by ELISA. PK parameters were calculated using noncompartmental curve stripping methods of PK Solutions 2.0 (Summit Research Services, Montrose, CO).

Validation of resuscitated PRL-humanized mice

Female PRL-humanized mice (B6.Cg-Prl^{tm1Hmn} Tg(PRL) 30Greg/Mmmh) were anesthetized with isoflurane (2%) and whole blood was collected by cardiac puncture and coagulated at room temperature for one hour before isolating serum by centrifugation at 6,000 rcf, 10 min, 4°C. Serum samples were collected and stored at −80°C until use. Serum levels of PRL species were quantified using a mPRL or hPRL ELISA kit according to manufacturer's instructions (Abcam, #ab100736; NovusBio, #NBP2–60128, respectively).

Hindpaw tactile allodynia assessment

Female PRL-humanized mice were treated with either PL 200,019 (20 mg/kg, SC) or vehicle (PBS, 10 mL/kg, SC) on day 0, followed by 2-hour RS sessions repeated on three consecutive days (*i.e.*, days 1, 2, 3). Hindpaw mechanical allodynia was assessed using von Frey filament before (baseline, on day 1) and after the three RS sessions (*i.e.*, days 3, 5, 7, 10, 12 and 14). For RS sessions, animals were placed in individual plastic restrainers (Plas-labs Inc., #551-BSRR), the mouse tail pulled through the stopper at the end of the tube, and the stopper pushed tightly enough against the animals to limit movement without inhibiting respiration. Animals were observed continuously during stress exposure. Hindpaw tactile allodynia was assessed as described previously,[85] the mice were acclimated for two hours individually in clear Plexiglas chambers (3 × 3 × 7inch) wrapped with black poster board on elevated wire-mesh platforms to allow access to the ventral surface of hindpaw. For response frequency measurement, a 1.0 g von Frey filament (Stoelting Co, #58011) was applied to the plantar surface of the hindpaw repeatedly and the number of times the mouse withdrew the paw was counted (10 trials at approximately 30 second intervals). Hindpaw withdrawal and licking were counted as positive responses to hindpaw stimulation. Animals were randomized to either drug or vehicle treatment. Investigators were blind to treatment. Five animals were used per group. Differences between drug- and vehicle-treated animals were assessed by Two-Way ANOVA with Sidak's test for multiple comparisons analysis using GraphPad Prism v9.4.1 (GraphPad Software, San Diego, CA).

Use of laboratory animals

PK studies were conducted at The Jackson Laboratory (Bar Harbor, ME), in research facilities fully accredited by the Association for Assessment and Accreditation of Laboratory Animal Care. Re-establishment of the PRL-humanized mouse colony (B6.Cg-*Prl*^{tm1Hmn} Tg(PRL)30Greg/Mmmh)[58] and pain studies in PRL-humanized mice were performed at the University of Arizona (Tucson, AZ). PK studies, reestablishment of the PRL-humanized mouse colony and pain studies were approved by corresponding Institutional Animal Care and Use Committees.

Abbreviations

ADCC	antibody-dependent cellular cytotoxicity
ADCP	antibody-dependent cellular phagocytosis
CDR	Complementarity-determining regions
D2	Dopaminergic type 2
DRG	Dorsal root ganglia
EC_{50}	Half-maximal effective concentration
ELISA	Enzyme-linked immunosorbent assay
Fc	Fragment crystallizable
FcγR	Fragment crystallizable gamma receptor
FPS:	Functional pain syndromes
GH	Growth hormone
HC	Heavy chain
Hgh	Human growth hormone
hPL	Human placental lactogen
HPLC	High performance liquid chromatography
hPRL	Human prolactin
hPRLR	Human prolactin receptor
IC_{50}	Half-maximal inhibitory concentration
IND	Investigational New Drug application
IV	Intravenous
K_D	equilibrium dissociation constant
k_{off}	Disassociation rate constant
k_{on}	Association rate constant
LC	Light chain
LCMS	Liquid chromatography mass spectrometry
mAb	Monoclonal antibody
MBP	Maltose binding protein
MOA	Mechanism of action
mPRL	Mouse prolactin
mPRLR	Mouse prolactin receptor
nhpPRL	Non-human primate prolactin
PBS	Phosphate-buffered saline
PBST	Phosphate-buffered saline with 0.05% Tween-20
PK	Pharmacokinetic
PL	Placental lactogen
PRL mAb	Humanized prolactin neutralizing monoclonal antibody
PRL	Prolactin
PRLR	Prolactin receptor
RLU	Relative bioluminescence signal
RP	Reverse phase
rPRL	Rat prolactin
RS	Restraint stress
SC	Subcutaneous
SEC	Size exclusion chromatography
TFA	Trifluoroacetic acid
TG	Trigeminal ganglion
TR-FRET	Time-resolved fluorescence energy transfer
VH	Variable heavy
VL	Variable light

Acknowledgments

The authors are grateful for the support of the Molecular Mass Spectrometry Facility at the University of California, San Diego (San Diego, CA) and The Jackson Laboratory (Bar Arbor, ME).

Disclosure statement

SM, GB, KW, CDS, SMG, and PR are present or former employees or consultants for Peptide Logic LLC.

Funding

This work was supported by NIH grants [R43NS122700] and [R01NS120395].

ORCID

Pierre J.M. Rivière http://orcid.org/0000-0002-8844-9130

References

1. Bartley EJ, Fillingim RB. Sex differences in pain: a brief review of clinical and experimental findings. Br J Anaesth. 2013;111:52–58. doi:10.1093/bja/aet127. PMID: 23794645.
2. Navratilova E, Fillingim RB, Porreca F. Sexual dimorphism in functional pain syndromes. Sci Transl Med. 2021;13:eabj7180. doi:10.1126/scitranslmed.abj7180. PMID: 34757805.
3. Hoffmann RG, Kotchen JM, Kotchen TA, Cowley T, Dasgupta M, Cowley AW Jr. Temporomandibular disorders and associated clinical comorbidities. Clin J Pain. 2011;27(3):268–74. doi:10.1097/AJP.0b013e31820215f5. PMID: 21178593.
4. Lipton RB, Stewart WF, Diamond S, Diamond ML, Reed M. Prevalence and burden of migraine in the United States: data from the American migraine study II. Headache. 2001;41(7):646–57. doi:10.1046/j.1526-4610.2001.041007646.x. PMID: 11554952.
5. Sandler RS. Epidemiology of irritable bowel syndrome in the United States. Gastroenterology. 1990;99(2):409–15. doi:10.1016/0016-5085(90)91023-y. PMID: 2365191.
6. Yunus MB. The role of gender in fibromyalgia syndrome. Curr Rheumatol Rep. 2001;3(2):128–34. PMID: 11286669. doi:10.1007/s11926-001-0008-3.
7. Bornstein J, Preti M, Simon JA, As-Sanie S, Stockdale CK, Stein A, Parish SJ, Radici G, Vieira-Baptista P, Pukall C, et al. Descriptors of Vulvodynia: A multisocietal definition consensus (International Society for the study of Vulvovaginal disease, the International Society for the study of women sexual health, and the International Pelvic pain Society). J Low Genit Tract Dis. 2019;23(2):161–63. doi:10.1097/LGT.0000000000000461. PMID: 30768446.
8. Fuldeore MJ, Soliman AM. Prevalence and symptomatic burden of diagnosed endometriosis in the United States: National estimates from a cross-sectional survey of 59,411 women. Gynecol Obstet Invest. 2017;82(5):453–61. PMID: 27820938. doi:10.1159/000452660.
9. Klein JR, Litt IF. Epidemiology of adolescent dysmenorrhea. Pediatrics. 1981;68(5):661–64. doi:10.1542/peds.68.5.661. PMID: 7312467.

10. MacGregor EA. Migraine and the menopause. J Br Menopause Soc. 2006;12:104–08. doi:10.1258/136218006778234048. PMID: 16953983.
11. Vetvik KG, Macgregor EA, Lundqvist C, Russell MB. Prevalence of menstrual migraine: a population-based study. Cephalalgia. 2014;34 (4):280–88. doi:10.1177/0333102413507637. PMID: 24101732.
12. Slatculescu AM, Chen Y. Synergism between female gender and high levels of daily stress associated with migraine Headaches in Ontario, Canada. Neuroepidemiology. 2018;51(3–4):183–89. doi:10.1159/000492503. PMID: 30153678.
13. Takeda T, Tadakawa M, Koga S, Nagase S, Yaegashi N. Relationship between dysmenorrhea and posttraumatic stress disorder in Japanese high school students 9 months after the Great East Japan Earthquake. J Pediatr Adolesc Gynecol. 2013;26:355–57. doi:10.1016/j.jpag.2013.06.020. PMID: 24075088.
14. Brasil DL, Montagna E, Trevisan CM, La Rosa VL, Lagana AS, Barbosa CP, Bianco B, Zaia V. Psychological stress levels in women with endometriosis: systematic review and meta-analysis of observational studies. Minerva Med. 2020;111(1):90–102. doi:10.23736/S0026-4806.19.06350-X. PMID: 31755674.
15. Chen Y, Moutal A, Navratilova E, Kopruszinski C, Yue X, Ikegami M, Chow M, Kanazawa I, Bellampalli SS, Xie J, et al. The prolactin receptor long isoform regulates nociceptor sensitization and opioid-induced hyperalgesia selectively in females. Sci Transl Med. 2020;12(529):12. doi:10.1126/scitranslmed.aay7550. PMID: 32024801.
16. Chen Y, Navratilova E, Dodick DW, Porreca F. An emerging role for prolactin in female-selective pain. Trends Neurosci. 2020;43 (8):635–48. doi:10.1016/j.tins.2020.06.003. PMID: 32620290.
17. Belugin S, Diogenes AR, Patil MJ, Ginsburg E, Henry MA, Akopian AN. Mechanisms of transient signaling via short and long prolactin receptor isoforms in female and male sensory neurons. J Biol Chem. 2013;288:34943–55. doi:10.1074/jbc.M113.486571. PMID: 24142695.
18. Diogenes A, Patwardhan AM, Jeske NA, Ruparel NB, Goffin V, Akopian AN, Hargreaves KM. Prolactin modulates TRPV1 in female rat trigeminal sensory neurons. J Neurosci. 2006;26 (31):8126–36. doi:10.1523/JNEUROSCI.0793-06.2006. PMID: 16885226.
19. Patil M, Hovhannisyan AH, Wangzhou A, Mecklenburg J, Koek W, Goffin V, Grattan D, Boehm U, Dussor G, Price TJ, et al. Prolactin receptor expression in mouse dorsal root ganglia neuronal subtypes is sex-dependent. J Neuroendocrinol. 2019;31 (8):e12759. doi:10.1111/jne.12759. PMID: 31231869.
20. Patil M, Belugin S, Mecklenburg J, Wangzhou A, Paige C, Barba-Escobedo PA, Boyd JT, Goffin V, Grattan D, Boehm U, et al. Prolactin regulates pain responses via a female-selective nociceptor-specific mechanism. iScience. 2019;20:449–65. doi:10.1016/j.isci.2019.09.039. PMID: 31627131.
21. Patil MJ, Green DP, Henry MA, Akopian AN. Sex-dependent roles of prolactin and prolactin receptor in postoperative pain and hyperalgesia in mice. Neuroscience. 2013;253:132–41. doi:10.1016/j.neuroscience.2013.08.035. PMID: 23994182.
22. Patil MJ, Ruparel SB, Henry MA, Akopian AN. Prolactin regulates TRPV1, TRPA1, and TRPM8 in sensory neurons in a sex-dependent manner: Contribution of prolactin receptor to inflammatory pain. Am J Physiol Endocrinol Metab. 2013;305(9): E1154–E64. doi:10.1152/ajpendo.00187.2013. PMID: 24022869.
23. Scotland PE, Patil M, Belugin S, Henry MA, Goffin V, Hargreaves KM, Akopian AN. Endogenous prolactin generated during peripheral inflammation contributes to thermal hyperalgesia. Eur J Neurosci. 2011;34:745–54. doi:10.1111/j.1460-9568.2011.07788.x. PMID: 21777304.
24. Al-Karagholi MA, Kalatharan V, Ghanizada H, Dussor G, Ashina M. Prolactin in headache and migraine: A systematic review of preclinical studies. Headache. 2023;63(5):577–84. doi:10.1111/head.14412. PMID: 36752584.
25. Goffin V, Binart N, Touraine P, Kelly PA. Prolactin: the new biology of an old hormone. Annu Rev Physiol. 2002;64(1):47–67. doi:10.1146/annurev.physiol.64.081501.131049. PMID: 11826263.
26. Bernard V, Young J, Binart N. Prolactin — a pleiotropic factor in health and disease. Nat Rev Endocrinol. 2019;15(6):356–65. doi:10.1038/s41574-019-0194-6. PMID: 30899100.
27. Marano RJ, Ben-Jonathan N. Minireview: Extrapituitary prolactin: an update on the distribution, regulation, and functions. Molecular Endocrinology. 2014;28(5):622–33. doi:10.1210/me.2013-1349. PMID: 24694306.
28. Lennartsson AK, Jonsdottir IH. Prolactin in response to acute psychosocial stress in healthy men and women. Psychoneur oendocrinology. 2011;36(10):1530–39. doi:10.1016/j.psyneuen.2011.04.007. PMID: 21621331.
29. Tanner MJ, Hadlow NC, Wardrop R. Variation of female prolactin levels with menopausal status and phase of menstrual cycle. Aust N Z J Obstet Gynaecol. 2011;51:321–24. doi:10.1111/j.1479-828X.2011.01321.x. PMID: 21806583.
30. Bernichtein S, Touraine P, Goffin V. New concepts in prolactin biology. J Endocrinol. 2010;206:1–11. doi:10.1677/JOE-10-0069. PMID: 20371569.
31. Al-Karagholi MA, Kalatharan V, Ghanizada H, Gram C, Dussor G, Ashina M. Prolactin in headache and migraine: A systematic review of clinical studies. Cephalalgia. 2023;43(2):3331024221136286. doi:10.1177/03331024221136286. PMID: 36718026.
32. Auriemma RS, Del Vecchio G, Scairati R, Pirchio R, Liccardi A, Verde N, de Angelis C, Menafra D, Pivonello C, Conforti A, et al. The Interplay between prolactin and reproductive System: Focus on Uterine pathophysiology. Front Endocrinol (Lausanne). 2020;11:594370. doi:10.3389/fendo.2020.594370. PMID: 33162942.
33. Bussone G, Usai S, Moschiano F. How to investigate and treat: headache and hyperprolactinemia. Curr Pain Headache Rep. 2012;16 (4):365–70. doi:10.1007/s11916-012-0267-x. PMID: 22639180.
34. Courtillot C, Plu-Bureau G, Binart N, Balleyguier C, Sigal-Zafrani B, Goffin V, Kuttenn F, Kelly PA, Touraine P. Benign breast diseases. J Mammary Gland Biol Neoplasia. 2005;10(4):325–35. doi:10.1007/s10911-006-9006-4. PMID: 16900392.
35. De Hert M, Detraux J, Stubbs B. Relationship between antipsychotic medication, serum prolactin levels and osteoporosis/osteoporotic fractures in patients with schizophrenia: a critical literature review. Expert Opin Drug Saf. 2016;15:809–23. doi:10.1517/14740338.2016.1167873. PMID: 26986209.
36. Hirschowitz JS, Soler NG, Wortsman J. The galactorrhoea-endometriosis syndrome. Lancet. 1978;311(8070):896–98. doi:10.1016/s0140-6736(78)90679-7. PMID: 76843.
37. Rastrelli G, Corona G, Maggi M. The role of prolactin in andrology: what is new? Rev Endocr Metab Disord. 2015;16(3):233–48. doi:10.1007/s11154-015-9322-3. PMID: 26542707.
38. Watanabe M, Kopruszinski CM, Moutal A, Ikegami D, Khanna R, Chen Y, Ross S, Mackenzie K, Stratton J, Dodick DW, et al. Dysregulation of serum prolactin links the hypothalamus with female nociceptors to promote migraine. Brain. 2022;145 (8):2894–909. doi:10.1093/brain/awac104. PMID: 35325034.
39. Avona A, Mason BN, Burgos-Vega C, Hovhannisyan AH, Belugin SN, Mecklenburg J, Goffin V, Wajahat N, Price TJ, Akopian AN, et al. Meningeal CGRP-Prolactin interaction evokes female-specific migraine behavior. Ann Neurol. 2021;89 (6):1129–44. doi:10.1002/ana.26070. PMID: 33749851.
40. Kallestrup MM, Kasch H, Osterby T, Nielsen E, Jensen TS, Jorgensen JO. Prolactinoma-associated headache and dopamine agonist treatment. Cephalalgia. 2014;34(7):493–502. doi:10.1177/0333102413515343. PMID: 24351278.
41. Noori-Zadeh A, Karamkhani M, Seidkhani-Nahal A, Khosravi A, Darabi S. Evidence for hyperprolactinemia in migraineurs: a systematic review and meta-analysis. Neurol Sci. 2020;41(1):91–99. doi:10.1007/s10072-019-04035-7. PMID: 31444732.
42. Oliveira MDC, Barea LM, Horn APK, Ongaratti BR, Soares JOD, Araujo B, Santos TMD, Rech CL, Pereira-Lima JFS. Resolution of headache after reduction of prolactin levels in hyperprolactinemic patients. Arq Neuropsiquiatr. 2020;78(1):28–33. doi:10.1590/0004-282X20190143. PMID: 32074187.

43. Gerlo S, Davis JR, Mager DL, Kooijman R. Prolactin in man: a tale of two promoters. Bioessays. 2006;28(10):1051–55.doi:10.1002/bies.20468. PMID: 16998840.
44. Goffin V, Touraine P, Culler MD, Kelly PA. Drug insight: prolactin-receptor antagonists, a novel approach to treatment of unresolved systemic and local hyperprolactinemia? Nat Clin Pract Endocrinol Metab. 2006;2(10):571–81. doi:10.1038/ncpendmet0270. PMID: 17024156.
45. Liu T, Joo SH, Voorhees JL, Brooks CL, Pei D. Synthesis and screening of a cyclic peptide library: discovery of small-molecule ligands against human prolactin receptor. Bioorg Med Chem. 2009;17(3):1026–33. doi:10.1016/j.bmc.2008.01.015. PMID: 18234500.
46. Otto C, Sarnefalt A, Ljungars A, Wolf S, Rohde-Schulz B, Fuchs I, Schkoldow J, Mattsson M, Vonk R, Harrenga A, et al. A neutralizing prolactin receptor antibody Whose in vivo application Mimics the phenotype of female prolactin receptor-deficient mice. Endocrinology. 2015;156(11):4365–73. doi:10.1210/en.2015-1277. PMID: 26284426.
47. Damiano JS, Rendahl KG, Karim C, Embry MG, Ghoddusi M, Holash J, Fanidi A, Abrams TJ, Abraham JA. Neutralization of prolactin receptor function by monoclonal antibody LFA102, a novel potential therapeutic for the treatment of breast cancer. Mol Cancer Ther. 2013;12(3):295–305. doi:10.1158/1535-7163.MCT-12-0886. PMID: 23270929.
48. Goffin V, Bernichtein S, Kayser C, Kelly PA. Development of new prolactin analogs acting as pure prolactin receptor antagonists. Pituitary. 2003;6(2):89–95. doi:10.1023/b:pitu.0000004799.41035.9f. PMID: 14703018.
49. Chen WY, Ramamoorthy P, Chen N, Sticca R, Wagner TE. A human prolactin antagonist, hPRL-G129R, inhibits breast cancer cell proliferation through induction of apoptosis. Clin Cancer Res. 1999;5:3583–93. https://www.ncbi.nlm.nih.gov/pubmed/10589775.
50. Yu S, Alkharusi A, Norstedt G, Graslund T, Henry KA. An in vivo half-life extended prolactin receptor antagonist can prevent STAT5 phosphorylation. PLoS One. 2019;14(5):e0215831. doi:10.1371/journal.pone.0215831. PMID: 31063493.
51. Goffin V, Shiverick KT, Kelly PA, Martial JA. Sequence-function relationships within the expanding family of prolactin, growth hormone, placental lactogen, and related proteins in mammals. Endocr Rev. 1996;17(4):385–410. doi:10.1210/edrv-17-4-385. PMID: 8854051.
52. Padros J, Chatel G, Caron M. Time-resolved Förster Resonance energy transfer assays for measurement of endogenous Phosphorylated STAT proteins in human cells. JoVe (J Visualized Exp). 2021;175. doi:10.3791/62915-v.PMID: 34570089.
53. Silva JP, Vetterlein O, Jose J, Peters S, Kirby H. The S228P mutation prevents in vivo and in vitro IgG4 Fab-arm exchange as demonstrated using a combination of novel quantitative immunoassays and physiological matrix preparation. J Biol Chem. 2015;290(9):5462–69. doi:10.1074/jbc.M114.600973. PMID: 25568323.
54. Yu J, Song Y, Tian W. How to select IgG subclasses in developing anti-tumor therapeutic antibodies. J Hematol Oncol. 2020;13(1):45. doi:10.1186/s13045-020-00876-4. PMID: 32370812.
55. Chenoweth AM, Wines BD, Anania JC, Mark Hogarth P. Harnessing the immune system via FcγR function in immune therapy: a pathway to next-gen mAbs. Immunol Cell Biol. 2020;98(4):287–304. doi:10.1111/imcb.12326. PMID: 32157732.
56. Avery LB, Wang M, Kavosi MS, Joyce A, Kurz JC, Fan YY, Dowty ME, Zhang M, Zhang Y, Cheng A, et al. Utility of a human FcRn transgenic mouse model in drug discovery for early assessment and prediction of human pharmacokinetics of monoclonal antibodies. MAbs. 2016;8(6):1064–78. doi:10.1080/19420862.2016.1193660. PMID: 27232760.
57. Mason BN, Kallianpur R, Price TJ, Akopian AN, Dussor GO. Prolactin signaling modulates stress-induced behavioral responses in a preclinical mouse model of migraine. Headache. 2022;62(1):11–25. doi:10.1111/head.14248. PMID: 34967003.
58. Christensen HR, Murawsky MK, Horseman ND, Willson TA, Gregerson KA. Completely humanizing prolactin rescues infertility in prolactin knockout mice and leads to human prolactin expression in extrapituitary mouse tissues. Endocrinology. 2013;154(12):4777–89. doi:10.1210/en.2013-1476. PMID: 24029242.
59. Utama FE, LeBaron MJ, Neilson LM, Sultan AS, Parlow AF, Wagner KU, Rui H. Human prolactin receptors are insensitive to mouse prolactin: implications for xenotransplant modeling of human breast cancer in mice. J Endocrinol. 2006;188(3):589–601. doi:10.1677/joe.1.06560. PMID: 16522738.
60. Roopenian DC, Low BE, Christianson GJ, Proetzel G, Sproule TJ, Wiles MV. Albumin-deficient mouse models for studying metabolism of human albumin and pharmacokinetics of albumin-based drugs. MAbs. 2015;7(2):344–51. doi:10.1080/19420862.2015.1008345. PMID: 25654695.
61. Nakamura G, Ozeki K, Takesue H, Tabo M, Hosoya KI. Prediction of human pharmacokinetics profile of monoclonal antibody using hFcrn transgenic mouse model. Biol Pharm Bull. 2021;44:389–95. doi:10.1248/bpb.b20-00775. PMID: 33642546.
62. Betts A, Keunecke A, van Steeg TJ, van der Graaf PH, Avery LB, Jones H, Berkhout J, van Steeg TJ, van der Graaf PH. Linear pharmacokinetic parameters for monoclonal antibodies are similar within a species and across different pharmacological targets: A comparison between human, cynomolgus monkey and hFcrn Tg32 transgenic mouse using a population-modeling approach. MAbs. 2018;10(5):751–64. doi:10.1080/19420862.2018.1462429. PMID: 29634430.
63. Bruhns P, Jonsson F. Mouse and human FcR effector functions. Immunol Rev. 2015;268(1):25–51. doi:10.1111/imr.12350. PMID: 26497511.
64. Otto C, Wolf S, Freiberg C, Harrenga A, Greven S, Trautwein M, Bruder S, Eicker A, Wilen A. Neutralizing prolactin receptor antibodies and their therapeutic use. WO 2011/069799 A1. World Intellectual Property Organization; 2011.
65. Kelly PA, Binart N, Freemark M, Lucas B, Goffin V, Bouchard B. Prolactin receptor signal transduction pathways and actions determined in prolactin receptor knockout mice. Biochem Soc Trans. 2001;29(2):48–52. doi:10.1042/0300-5127:0290048. PMID: 11356125.
66. LaPensee CR, Horseman ND, Tso P, Brandebourg TD, Hugo ER, Ben-Jonathan N. The prolactin-deficient mouse has an unaltered metabolic phenotype. Endocrinology. 2006;147(10):4638–45. doi:10.1210/en.2006-0487. PMID: 16809445.
67. Lee GJ, Porreca F, Navratilova E. Prolactin and pain of endometriosis. Pharmacology & Therapeutics. 2023;247:108435. doi:10.1016/j.pharmthera.2023.108435. PMID: 37169264.
68. De LD, Becerra A, Lahera M, JI B, Valero VC, Varela C. A randomized cross-over study comparing cabergoline and quinagolide in the treatment of hyperprolactinemic patients. J Endocrinol Invest. 2000;23(7):428–34. doi:10.1007/BF03343751. PMID: 11005266.
69. FDA. Labelling-Package insert for New Drug application (NDA): 020664. Updated 12/13/2019, FDA, drugs@FDA; 1996.
70. Leanos-Miranda A, Pascoe-Lira D, Chavez-Rueda KA, Blanco-Favela F. Antiprolactin autoantibodies in systemic lupus erythematosus: frequency and correlation with prolactinemia and disease activity. J Rheumatol. 2001;28(7):1546–53. https://www.ncbi.nlm.nih.gov/pubmed/11469460. PMID: 11469460.
71. Blanco-Favela F, Quintal Ma G, Chavez-Rueda AK, Leanos-Miranda A, Berron-Peres R, Baca-Ruiz V, Lavalle-Montalvo C. Anti-prolactin autoantibodies in paediatric systemic lupus erythematosus patients. Lupus. 2001;10(11):803–08. doi:10.1177/096120330101001107. PMID: 11789490.
72. Leanos-Miranda A, Chavez-Rueda KA, Blanco-Favela F. Biologic activity and plasma clearance of prolactin-IgG complex in patients with systemic lupus erythematosus. Arthritis & Rheumatism. 2001;44:866–75. doi:10.1002/1529-013120010444:4<866:AID-ANR143>3.0.CO;2-6. PMID: 11315926.
73. FDA. CDER review for new drug application (NDA): 020664. FDA, Drugs@FDA. 1996.
74. Stubenrauch K, Wessels U, Regula JT, Kettenberger H, Schleypen J, Kohnert U. Impact of molecular processing in the hinge region of therapeutic IgG4 antibodies on disposition profiles

in cynomolgus monkeys. Drug Metab Dispos. 2010;38(1):84–91. doi:10.1124/dmd.109.029751. PMID: 19850673.
75. Lewis KB, Meengs B, Bondensgaard K, Chin L, Hughes SD, Kjaer B, Lund S, Wang L. Comparison of the ability of wild type and stabilized human IgG(4) to undergo Fab arm exchange with endogenous IgG(4)in vitro and in vivo. Mol Immunol. 2009;46(16):3488–94. doi:10.1016/j.molimm.2009.07.009. PMID: 19683345.
76. Wang C, Thudium KB, Han M, Wang XT, Huang H, Feingersh D, Garcia C, Wu Y, Kuhne M, Srinivasan M, et al. In vitro characterization of the anti-PD-1 antibody nivolumab, BMS-936558, and in vivo toxicology in non-human primates. Cancer Immunol Res. 2014;2(9):846–56. doi:10.1158/2326-6066.CIR-14-0040. PMID: 24872026.
77. Yang X, Wang F, Zhang Y, Wang L, Antonenko S, Zhang S, Zhang YW, Tabrizifard M, Ermakov G, Wiswell D, et al. Comprehensive analysis of the therapeutic IgG4 antibody pembrolizumab: hinge modification blocks half molecule exchange in vitro and in vivo. J Pharm Sci. 2015;104(12):4002–14. doi:10.1002/jps.24620. PMID: 26308749.
78. Nath N, Godat B, Flemming R, Urh M. A homogeneous bioluminescent immunoassay for parallel characterization of binding between a panel of antibodies and a family of Fcγ receptors. Sci Rep. 2022;12(1):12185. doi:10.1038/s41598-022-15887-z. PMID: 35842448.
79. Chai Q, Shih J, Weldon C, Phan S, Jones BE. Development of a high-throughput solubility screening assay for use in antibody discovery. MAbs. 2019;11(4):747–56. doi:10.1080/19420862.2019.1589851. PMID: 30913963.
80. Abanades B, Wong WK, Boyles F, Georges G, Bujotzek A, CM D. ImmuneBuilder: Deep-Learning models for predicting the structures of immune proteins. bioRxiv. 2022;2022 2011.2004.514231. doi:10.1101/2022.11.04.514231.
81. Raybould MIJ, Marks C, Krawczyk K, Taddese B, Nowak J, Lewis AP, Bujotzek A, Shi J, Deane CM. Five computational developability guidelines for therapeutic antibody profiling. Proc Natl Acad Sci U S A. 2019;116:4025–30. doi:10.1073/pnas.1810576116. PMID: 30765520.
82. Gao SH, Huang K, Tu H, Adler AS. Monoclonal antibody humanness score and its applications. BMC Biotechnol. 2013;13:55. doi:10.1186/1472-6750-13-55. PMID: 23826749.
83. Kozlowski LP. IPC – Isoelectric Point Calculator. Biol Direct. 2016;11(1):55. doi:10.1186/s13062-016-0159-9.
84. Grimsley GR, Scholtz JM, Pace CN. A summary of the measured pK values of the ionizable groups in folded proteins. Protein Sci. 2009;18:247–51. doi:10.1002/pro.19. PMID: 19177368.
85. Chaplan SR, Bach FW, Pogrel JW, Chung JM, Yaksh TL. Quantitative assessment of tactile allodynia in the rat paw. J Neurosci Methods. 1994;53(1):55–63. doi:10.1016/0165-0270(94)90144-9. PMID: 7990513.